

Superconducting qubits can be coupled and addressed as trapped ions

Yu-xi Liu,¹ L. F. Wei,¹ J. S. Tsai,^{1,2} and Franco Nori^{1,3}

¹Frontier Research System, The Institute of Physical and Chemical Research (RIKEN), Wako-shi 351-0198, Japan

²NEC Fundamental Research Laboratories, Tsukuba Ibaraki 305-8051, Japan

³Center for Theoretical Physics, Physics Department, Center for the Study of Complex Systems, The University of Michigan, Ann Arbor, Michigan 48109-1040, USA

(Dated: February 8, 2020)

We propose a scalable circuit with superconducting qubits (SCQs) which is essentially the same as the successful one now being used for trapped ions. The SCQs act as “trapped ions” and are coupled to a “vibrating” mode provided by a superconducting LC circuit—the data bus (DB). Each SCQ can be separately addressed by an applied time-dependent magnetic flux (TDMF). Single-qubit rotations and qubit-DB couplings/decouplings are controlled by the frequencies of the TDMFs. Thus, qubit-qubit interactions, mediated by the DB, can be selectively performed. The implementation of logic gates and the transfer of information using this circuit are also investigated.

PACS numbers: 03.67.Lx, 74.50.+r, 85.25.Cp

Introduction.— Superconducting quantum circuits with Josephson junctions are currently studied for their potential applications in quantum information processing. Experiments have been performed using charge [1, 2], flux [3], phase [4], and charge-flux [5] superconducting qubits (SCQs). Quantum coherent oscillations and conditional gate operations have been demonstrated using two coupled superconducting charge qubits [6]. For a circuit with two coupled flux qubits, spectroscopic measurements show that it acts as a quantum mechanical four-level system [7]. Further, entangled macroscopic quantum states have been experimentally verified in coupled flux [8], and phase [9, 10, 11] qubits.

A major challenge for SCQs is how to design an experimentally realizable circuit where the couplings for different qubits can be selectively switched on and off, and then scaled up to many qubits. Current experiments [6, 7, 8, 9, 10, 11], with *always-on interbit couplings*, make circuits difficult to scale up. Theoretical proposals (e.g., Refs. [12, 13, 14, 15]) have been put forward to selectively couple any pair of qubits through a common data bus (DB). Some proposals (e.g., Refs. [12, 13]) only involve virtual excitations of the DB modes, while in others (e.g., Refs. [14, 15]), the DB modes need to be excited. In the former case [12, 13], the effective qubit couplings can be switched on and off by changing the magnetic flux through the circuit. In practice, the switchable coupling means that the sudden switching time of the magnetic flux through the loop should be less than \hbar/E_J (here, E_J is the single-qubit Josephson energy). This is a challenge for current experiments. In the later case [14, 15], the qubit and the DB are required to have the same (resonant) eigenfrequencies when they are coupled. When one of their frequencies is suddenly changed, such that the qubit and the DB have a large detuning (i.e., the non-resonant regime), then, they are decoupled. However, the non-adiabatic change of the eigenfrequencies introduces more noise and makes the qubit and the DB unstable during the fast quantum computing operations.

We now propose a different approach to realize scalable SCQs. Here, the individual properties (e.g., eigenfrequencies)

of the DB and qubits are *always fixed*, but the qubit-DB *couplings* can be conveniently *controlled by changing the frequencies* of the applied time-dependent magnetic fluxes (TDMFs). Our controllable coupling mechanism is also different from the recent one in Ref. [16] although, in both proposals, the TDMFs are used to assist the coupling and decoupling. There, the uncoupled qubits are coupled through the dressed states formed by the TDMFs and the qubit. Here, the coupling is realized by compensating the qubit-DB energy difference using selected frequencies of the TDMFs on the qubits. Our proposal can be essentially reduced to the one used for trapped ions [17], which means that the SCQs can be coupled and separately addressed similarly to trapped ions. This is very significant because trapped ions [17, 18] are further ahead, along the quantum computing Roadmap, of other qubits.

Model.— We consider flux qubits (using a loop with either three junctions [3] or one junction [19]). Without loss of generality, the simplest circuit is considered, as shown in Fig. 1, where two flux qubits are coupled to an LC circuit (acting as a DB) with inductance L and capacitance C . The mutual inductance between the l th qubit and the LC circuit is $M^{(l)}$, with $l = 1, 2$. The applied magnetic flux $\Phi^{(l)}$ through the l th qubit loop is assumed to include a static (or dc) magnetic flux $\Phi_e^{(l)}$ and a time-dependent magnetic flux (TDMF) $\Phi_e^{(l)}(t) = A_l \cos(\omega_c^{(l)} t)$, with real amplitude A_l and frequency $\omega_c^{(l)}$. Thus the Hamiltonian can be written as

$$H = \sum_{l=1}^2 H_l + \frac{Q^2}{2C} + \frac{\phi^2}{2L} + \sum_{l=1}^2 IM^{(l)} I^{(l)}, \quad (1)$$

where the mutual inductance between the two qubits has been neglected. The variable I and $\phi = IL$ are the current and magnetic flux through the LC circuit. We first consider a three-junction qubit; thus the Hamiltonian H_l in Eq. (1) should [20] be $H_l = \sum_{i=1}^3 (\Phi_0/2\pi) [(\Phi_0 C_{J_i}^{(l)}/\pi)(\dot{\varphi}_i^{(l)})^2 - I_{0i}^{(l)} \cos \varphi_i^{(l)}]$, after neglecting the qubit self-inductance and constant terms $I_{0i}^{(l)} \Phi_0/2\pi$. Each junction in the l th qubit

has a capacitance $C_{J_i}^{(l)}$, phase drop $\varphi_i^{(l)}$, and supercurrent $I_i^{(l)} = I_{0_i}^{(l)} \sin \varphi_i^{(l)}$ with critical current $I_{0_i}^{(l)}$. The loop current of the l th qubit is $I^{(l)} = C_l \sum_i (I_{0_i}^{(l)} / C_{J_i}^{(l)}) \sin \varphi_i^{(l)}$, where $C_l^{-1} = \sum_i (C_{J_i}^{(l)})^{-1}$, with the convention $C_{J_3}^{(l)} = \alpha C_{J_1}^{(l)} = \alpha C_{J_2}^{(l)}$, and $\alpha < 1$. The LC circuit can be treated as a harmonic oscillator with its creation $a^\dagger = (\omega C \phi - iQ) / \sqrt{2\hbar\omega C}$ and annihilation $a = (\omega C \phi + iQ) / \sqrt{2\hbar\omega C}$ operators corresponding to the frequency $\omega = 1/\sqrt{LC}$. Considering the TDMF, the phase constraint condition [21] through the l th qubit loop becomes $\sum_{i=1}^3 \varphi_i^{(l)} + 2\pi[f + (\Phi_e^{(l)}(t))/\Phi_0] = 0$ with the reduced bias flux $f = (\Phi_e^{(l)} - M^{(l)}I)/\Phi_0$, here the bias f includes the flux $M^{(l)}I$, produced by the LC circuit. Thus, in the qubit basis, the Hamiltonian in Eq. (1) becomes

$$\begin{aligned}
H = & \frac{\hbar}{2} \sum_{l=1}^2 \omega_q^{(l)} \sigma_z^{(l)} + \hbar\omega a^\dagger a + \sum_{l=1}^2 H_{\text{int}}^{(l)} \\
& + \sum_{l=1}^2 (\lambda_l \sigma_-^{(l)} + \text{h.c.})(e^{-i\omega_c^{(l)}t} + \text{h.c.}) \\
& - (a^\dagger + a) \sum_{l=1}^2 (\Omega_l \sigma_-^{(l)} + \text{h.c.})(e^{-i\omega_c^{(l)}t} + \text{h.c.}),
\end{aligned} \quad (2)$$

where the constant terms have been neglected, the Pauli operators of the l th qubit are defined as $\sigma_+^{(l)} = |e_l\rangle\langle g_l|$, $\sigma_-^{(l)} = |g_l\rangle\langle e_l|$, and $\sigma_z^{(l)} = |e_l\rangle\langle e_l| - |g_l\rangle\langle g_l|$. The computational basis states of the l th qubit are defined [21, 22], for $\Phi_e^{(l)}(t) = 0$, by two lowest eigenstates $|0\rangle_l = |g_l\rangle$ and $|1\rangle_l = |e_l\rangle$ of the Hamiltonian H_l with the two independent variables $\varphi_p^{(l)} = (\varphi_1^{(l)} + \varphi_2^{(l)})/2$ and $\varphi_m^{(l)} = (\varphi_1^{(l)} - \varphi_2^{(l)})/2$. The first two terms in Eq. (2) denote the free Hamiltonians of both qubits and the LC circuit; $\omega_q^{(l)}$ is the transition frequency between two basis states of the l th qubit. The always-on interaction Hamiltonian $H_{\text{int}}^{(l)}$ between the l th qubit and the DB in the third term of Eq. (2) is $H_{\text{int}}^{(l)} = \hbar(a^\dagger + a)(G_l \sigma_-^{(l)} + \text{h.c.})$ with the coupling constant $G_l = CM^{(l)}\sqrt{\hbar\omega/2L} \langle e_l | I_0^{(l)} | g_l \rangle$, where $I_0^{(l)}$ is the loop current of the l th qubit with $\Phi_e^{(l)}(t) = 0$. The fourth term represents the interaction between the l th qubit and its TDMF with the interaction strength $\lambda_l = A_l \langle e_l | I_3^{(l)} | g_l \rangle / 2$, here $I_3^{(l)}$ is the supercurrent of the third junction in the l th qubit loop when $\Phi_e^{(l)}(t) = 0$. The fifth term is the controllable nonlinear interaction among: the l th qubit, the DB, and the TDMF; with coupling strength $\Omega_l = B \langle e_l | E_{J_3}^{(l)}(\varphi_3^{(l)}) | g_l \rangle$ and $B = (A_l M^{(l)} C_l / 2 C_{J_3}^{(l)}) (2\pi/\Phi_0)^2 \sqrt{\hbar\omega/2L}$, where $E_{J_3}^{(l)}(\varphi_3^{(l)})$ is the Josephson energy of the third junction of the l th qubit with $\Phi_e^{(l)}(t) = 0$.

Realization of switchable qubit-DB interaction.— Comparing the Hamiltonian (2) with the one used in trapped ions [17, 18], we find that there are extra terms $H_{\text{int}}^{(l)}$ in our proposal for the superconducting circuit. However, when the circuit is initially fabricated, the detuning between the qubits and the DB can be chosen to be sufficiently large such that the con-

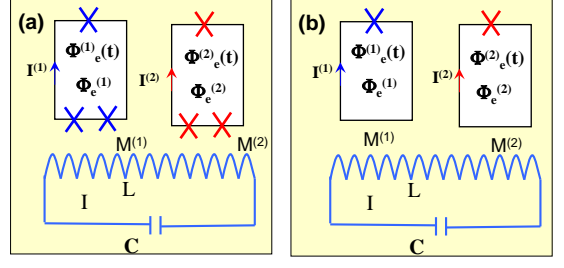


FIG. 1: (Color online) The l th flux qubit with three junctions in (a) or one junction in (b) is coupled to a LC circuit by the mutual inductance $M^{(l)}$ ($l=1,2$). An externally applied magnetic flux through the l th qubit includes a static (or dc) part $\Phi_e^{(l)}$ and the time-dependent part $\Phi_e^{(l)}(t)$. The currents through the first, the second qubits, and LC circuit are $I^{(1)}$, $I^{(2)}$, and I respectively. The two different external microwave fields $\Phi_e^{(l)}(t)$ can be used to control the couplings between the LC circuit and the different qubits. The bottom LC circuit can be replaced either by a transmission line resonator or by a loop with one junction (which acts as an inductance and has a capacitance).

dition $\Delta_l = \omega_q^{(l)} - \omega \gg |G_l|$ is satisfied, e.g., $|G_l|/\Delta_l \ll 1$. Therefore, the qubit-DB always-on interaction terms denoted by $H_{\text{int}}^{(l)}$ can be neglected [11]. Thus, the Hamiltonian (2) now has the same form as the one used for quantum computing with trapped ions, in the Lamb-Dicke limit [17, 18]. Here, the SCQs act as “trapped ions” and are coupled to a common “vibrating” mode formed by the LC circuit. Each SCQ can be separately addressed by the TDMF.

Analogous to the case of trapped ions, three-types of dynamical evolutions can be produced by using the frequency-matching (resonant) condition: i) if $\omega_c^{(l)} = \omega_q^{(l)}$, the qubit and the DB evolve independently. The external flux $\Phi_e^{(l)}(t)$ is only used to separately address the l th qubit rotations. These rotations are governed by the Hamiltonian $H_c^{(l)} = \lambda_l \sigma_-^{(l)} + \text{h.c.}$, in the interaction picture (IP) and using the rotating-wave approximation (RWA) (also for the $H_r^{(l)}$ and $H_b^{(l)}$ shown below). This is the so-called “carrier process” in the trapped ions approach. ii) If the frequencies satisfy the condition $\omega_c^{(l)} = \omega_q^{(l)} - \omega$, then the $\Phi_e^{(l)}(t)$ assists the l th qubit to couple resonantly with the DB. This is the “red sideband” excitation, governed by the Hamiltonian $H_r^{(l)} = \Omega_l a^\dagger \sigma_-^{(l)} + \text{h.c.}$ iii) When the frequencies satisfy the condition $\omega_c^{(l)} = \omega_q^{(l)} + \omega$, it is the so-called “blue sideband” excitation: the l th qubit and the DB are coupled by the Hamiltonian $H_b^{(l)} = \Omega_l a \sigma_-^{(l)} + \text{h.c.}$

It is clear that the qubit-DB coupling (or decoupling) can be controlled by appropriately selecting the frequency $\omega_c^{(l)}$ of $\Phi_e^{(l)}(t)$ to match the above frequency condition, not by changing the eigenfrequency of the qubit or the DB. The properties (e.g., eigenfrequency) of the qubits and the DB are fixed when processing either the resonant coupling or the non-resonant decoupling. Also it is unnecessary to change the flux intensity through the qubit loop with a fast sweep rate. The only

requirement in our proposal is to change $\omega_c^{(l)}$.

Single- and two-qubit gates.— For the l th qubit, the carrier process described by the Hamiltonian $H_c^{(l)}$ can be used to perform the following single-qubit operation $U_c^{(l)}(\alpha_l, \phi_l) = \exp[-i\alpha_l(e^{-i\phi_l}\sigma_-^{(l)} + e^{i\phi_l}\sigma_+^{(l)})]$. Here, $\alpha_l = |\lambda_l|\tau$ depends on the Rabi frequency $|\lambda_l|/\hbar$ and duration τ ; ϕ_l is related to the phase of the TDMF applied to the l th qubit. For example, the phases $\phi_l = 0$ and $\phi_l = 3\pi/2$ correspond to the l th qubit rotations $R_x^{(l)}(\alpha_l)$ and $R_y^{(l)}(\alpha_l)$, about the x and y axis, respectively. Thus, any single-qubit operation can be implemented by a series of $R_x^{(l)}(\alpha_l)$ and $R_y^{(l)}(\alpha_l)$ operations with well-chosen different angles α_l .

Two-qubit gates can be obtained using two qubits interacting sequentially with their DB as in Ref. [17]. There, the controlled phase-flip and the controlled-NOT gates can be obtained by three and five steps, respectively. Here, we only discuss the difference between our proposal and the one used for trapped ions. In our circuit, the ratio $|G_l|/\Delta_l$ cannot be infinitely small. Then, the effect of the uncontrollable qubit-DB interaction $H_{\text{int}}^{(l)}$ needs to be considered by the effective Hamiltonian [23]

$$H_e^{(l)} = \hbar \frac{|G_l|^2}{\Delta_l} [|e_l\rangle\langle e_l| aa^\dagger - |g_l\rangle\langle g_l| a^\dagger a], \quad (3)$$

when the l th qubit is not addressed by the TDMF. After including this effect, three pulses (successively applied to the first, second, and first qubits) with durations τ_1 , τ_2 , and τ_3 (used to perform a controlled phase-flip gate in Ref. [17]) will result in a two-qubit gate U_{two} . This can be expressed as

$$U_{\text{two}} = \begin{pmatrix} 1 & 0 & 0 & 0 \\ 0 & \exp(-i\theta_1) & 0 & 0 \\ 0 & 0 & \exp(i\theta_2) & 0 \\ 0 & 0 & 0 & -\exp(-i\theta_3) \end{pmatrix} \quad (4)$$

in the two-qubit basis $\{|g_1\rangle|g_2\rangle, |g_1\rangle|e_2\rangle, |e_1\rangle|g_2\rangle, |e_1\rangle|e_2\rangle\}$ where $\theta_1 = 2|G_2|^2\tau_1/\Delta_2$, $\theta_2 = (|G_2|^2\tau_1/\Delta_2) + (|G_1|^2\tau_2/\Delta_1)$, and $\theta_3 = (3|G_2|^2\tau_1/\Delta_2) + (|G_1|^2\tau_2/\Delta_1)$. This shows that U_{two} is a controlled phase-flip gate for all $|G_l|/\Delta_l \sim 0$. Moreover, any quantum operation can also be realized by combining the two-qubit gate U_{two} with other single-qubit operations.

Entanglement and state transfer.— We now consider two different external fields satisfying frequency-matching conditions, e.g., red sideband excitation, which are simultaneously applied to the first two qubits in the left part of Fig. 2. Then in the IP and the RWA, the interaction Hamiltonian (2), between the LC circuit and the two qubits, is $H_1 = \sum_{l=1}^2 (\Omega a^\dagger \sigma_- + \text{h.c.})$. For simplicity, the coupling strengths between the LC circuit and different qubits are assumed to be identical, e.g., $\Omega_1 = \Omega_2 = |\Omega|e^{-i\theta}$. If the LC circuit is initially prepared in the first excited state $|1\rangle$, then the wave-function $|\Psi(t)\rangle$ of the whole system can be written as $|\Psi(t)\rangle = \cos(\sqrt{2}\Omega t)|g_1\rangle|g_2\rangle|1\rangle - ie^{i\theta} \sin(\sqrt{2}\Omega t)[|e_1\rangle|g_2\rangle|0\rangle + |g_1\rangle|e_2\rangle|0\rangle]$. When $\sqrt{2}\Omega t/\hbar =$

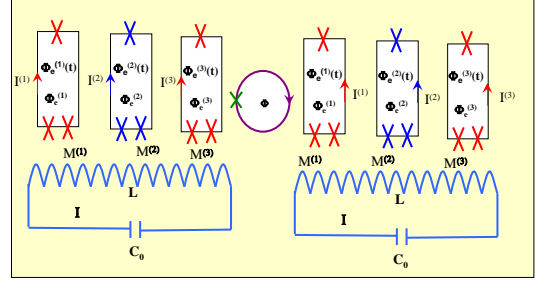


FIG. 2: (Color online) Two LC circuits with three junctions each. The information transfer among the two circuits is mediated by the middle superconducting loop with one junction. Even those here, three qubits are shown in one circuit, however, the number of qubits in each circuit can be much large.

$\pi/2$, then the LC circuit is in the vacuum state $|0\rangle$ and a maximally entangled state between two qubits can be generated as $|\Psi^+\rangle_{12} = [|e_1\rangle|g_2\rangle + |g_1\rangle|e_2\rangle]/\sqrt{2}$.

Using the three-qubit circuit shown on the left part of Fig. 2, let us discuss how an unknown state $|\psi\rangle = \beta_1|g_1\rangle + \beta_2|e_1\rangle$ in the first qubit can be transferred to the third one. We now consider the standard teleportation procedure: i) a maximally entangled state $|\Psi^+\rangle_{23} = [|e_2\rangle|g_3\rangle + |g_2\rangle|e_3\rangle]/\sqrt{2}$ between the second and third qubits is prepared by using the same method outlined above; ii) a CNOT gate $U_{\text{CNOT}}^{(12)}$ is implemented for the first and second qubits (here, the second one is the target); iii) a Hadamard gate is implemented on the first one; iv) simultaneous measurements, which can be done now in the superconducting circuits [11], are performed on the first and the second qubits. The four different measured results $|e_1, e_2\rangle$, $|e_1, g_2\rangle$, $|g_1, e_2\rangle$, and $|g_1, g_2\rangle$, correspond to the output states in the third qubit as $|\psi(e_1, e_2)\rangle$, $|\psi(e_1, g_2)\rangle$, $|\psi(g_1, e_2)\rangle$, and $|\psi(g_1, g_2)\rangle$. It can be easily found that the original state in the first one can be transferred to the third one when the measured result for the first and second qubits is $|e_1, e_2\rangle$. However, appropriate gates, e.g., $\sigma_x^{(3)}$, $\sigma_z^{(3)}$, and $\sigma_z^{(3)}\sigma_x^{(3)}$, need to be performed on the other three output states mentioned above. Afterwards, the state $|\psi\rangle_1$ can be transferred to the third qubit. The teleported states can be exactly known by virtue of the tomographic measurements on the output ones [24].

Experimentally accessible parameters.— We now analyze: (i) the always-on qubit-DB coupling $G_l \propto \langle e_l|I_0^{(l)}|g_l\rangle$, (ii) the TDMF driving Rabi frequency $\lambda_l \propto \langle e_l|\sin(2\varphi_p + 2\pi f)|g_l\rangle$, and (iii) the TDMF-controlled qubit-DB coupling $\Omega_l \propto \langle e_l|\cos(2\varphi_p + 2\pi f)|g_l\rangle$. In the single-qubit analysis [22], it is known that the qubit potential is symmetric at the degeneracy point $f = 1/2$, corresponding to well defined parities. A non-zero λ_l shows [22] that the qubit ground and excited states have opposite parities at $f = 1/2$. However, $\cos(2\varphi_p + 2\pi f)$ and the qubit loop current $I_0^{(l)}$ have even and odd parities, respectively, when $f = 1/2$. Then $\Omega_l = 0$ at the degeneracy point. In practice, $\Omega_l = 0$ can be avoided by slightly shifting f away from the degeneracy point

1/2. The controlled phase-flip gate also requires a transition from the ground state to the second excited state (an auxiliary level) [17]. It means that the bias flux f should be [22] near the degeneracy point, but $f \neq 1/2$.

For an experimentally accessible loop [3] current $\sim 0.5 \mu\text{A}$, the qubit frequency can be calculated [22, 25] to be $\Omega_q^{(l)}/2\pi = \nu_q^{(l)} \sim 4 \text{ GHz}$ and the Rabi frequency $\lambda_l/h \sim \nu_q^{(l)}/10$, near the degeneracy point. If the current through the LC circuit is of the same order as for the qubit, and the mutual inductances between the qubits and the DB are $\sim \text{pH}$, then the strengths G_l and Ω_l are around 300 MHz. The frequency differences between the qubits and the DB are usually about 1 to 10 GHz, then $|G_l/\Delta_l|$ is about 0.3 to 0.03. Therefore, the phase corrections θ_i , induced by the LC circuit, in Eq. (4) should be considered by using Eq. (3) for those qubits with $\Phi_e^{(l)}(t) = 0$.

For the LC circuit, if its capacitance C and inductance L are assumed as $\sim 10 \text{ fF}$ and $\sim 10 \text{ nH}$, respectively, then the LC circuit plasma frequency can be $\sim 10 \text{ GHz}$. The linear dimension for the LC circuit can be $\lesssim 1 \text{ cm}$. The estimated distance for negligible mutual inductance between two nearest qubits is $\sim 200 \mu\text{m}$, then one DB can approximately interact with ~ 40 qubits. Of course, the larger L of the LC circuit can have larger linear dimension, e.g., $L \sim 100 \text{ nH}$, and then more qubits, here about 400, can interact with the LC circuit. In practice, the superpositions of the ground and excited states for an LC circuit decay on a time scale given by $1/RC$, here R is the residual resistance of the circuit and its radiation losses. The larger LC circuit corresponds to a larger stray capacitance and resistance, and thus also corresponds to a shorter lifetime of the DB. For flux qubits, the dephasing time [26] is $\tau_\phi \approx 4 \mu\text{s}$ near the optimal point, which in principle should allow the information to be transferred more than one hundred qubits. If τ_ϕ can reach the estimated $20 \mu\text{s}$ (as in Ref. [27]), then the quantum information processing can be demonstrated using our circuit.

Conclusions.— We propose a scalable circuit with the SCQs coupled to a DB (an LC circuit), which can be operated similarly to trapped ions. In contrast to previous proposals (e.g., [12, 13, 14, 15]), the qubit-DB couplings/decouplings are controlled *neither* by changing the magnetic flux through the loop *nor* by changing the eigenfrequencies of the qubits (or the DB). They are *only* controlled via the *frequencies* of TDMFs. This is much easier to achieve in principle. In principle, the DB can couple tens of qubits. In order to further extend the scalability, we can use superconducting loops (each with one junction) to mediate and couple different circuits as shown in Fig. 2. We use three-junction flux qubits as an example to discuss our proposal; however, this method can be applied to other types of qubits, e.g., charge-flux [5], one-junction flux qubits [19]. Different from the three-junction ones, our proposal works well for these qubits [5, 19] at their optimal points [28].

We emphasize that: i) the LC circuit can be replaced by a transmission line resonator, or a superconducting circuit with one junction, or other similar elements. ii) If the DB is a one-

junction superconducting circuit, the TDMF, used to control the qubit-DB interaction, can be applied through the DB loop instead of applying it to the qubits. In this case, all qubits can work at their optimal points. iii) The TDMF can also be used to control [29] the flux-flux coupling through the mutual inductance for recent experiments [7, 8].

We thank J.Q. You, Y. Nakamura, Y.A. Pashkin, O. Astafiev, and K. Harrabi for their helpful discussions. This work was supported in part by the NSA and ARDA under AFOSR contract No. F49620-02-1-0334, and by the NSF grant No. EIA-0130383.

-
- [1] Y. Nakamura *et al.*, Nature, **398**, 786 (1999); K.W. Lehnert *et al.*, Phys. Rev. Lett. **90**, 027002 (2003).
 - [2] A. Wallraff *et al.*, Nature **431**, 162 (2004).
 - [3] C.J.M. Harmans *et al.*, Science **290**, 773 (2000); I. Chiorescu *et al.*, *ibid.* **299**, 1869 (2003).
 - [4] Y. Yu *et al.*, Science **296**, 889 (2002); J. Martinis *et al.*, Phys. Rev. Lett. **89**, 117901 (2002).
 - [5] D. Vion *et al.*, Science **296**, 886 (2002).
 - [6] Y.A. Pashkin *et al.*, Nature **421**, 823 (2003); T. Yamamoto *et al.*, *ibid.* **425**, 941 (2003).
 - [7] J.B. Majer *et al.*, Phys. Rev. Lett. **94**, 090501 (2005).
 - [8] A. Izmailkov *et al.*, Phys. Rev. Lett. **93**, 037003 (2004).
 - [9] H. Xu *et al.*, Phys. Rev. Lett. **94**, 027003 (2005).
 - [10] A.J. Berkley *et al.*, Science **300**, 1548 (2003).
 - [11] R. McDermott *et al.*, Science **307**, 1299 (2005).
 - [12] Y. Makhlin *et al.*, Rev. Mod. Phys. **73**, 357 (2001).
 - [13] J.Q. You *et al.*, Phys. Rev. Lett. **89**, 197902 (2002); Y.X. Liu *et al.*, Europhys. Lett. **67**, 941 (2004); L.F. Wei *et al.*, *ibid.* **67**, 1004 (2004); Phys. Rev. B **71**, 134506 (2005).
 - [14] A. Blais *et al.*, Phys. Rev. Lett. **90**, 127901 (2003); A. Blais *et al.*, Phys. Rev. A **69**, 062320 (2004).
 - [15] A.N. Cleland and M.R. Geller, Phys. Rev. Lett. **93**, 070501 (2004).
 - [16] C. Rigetti *et al.*, Phys. Rev. Lett. **94**, 240502 (2005).
 - [17] J.I. Cirac and P. Zoller, Phys. Rev. Lett. **74**, 4091 (1995).
 - [18] M. Sasura and V. Buzek, J. Mod. Opt. **49**, 1593 (2002).
 - [19] J.R. Friedman *et al.*, Nature **406**, 43 (2000).
 - [20] For the single-junction flux qubit, the Hamiltonian is $H_l = (P^2/2C_s) + U(\Phi, \Phi_x)$, with $P = -i\hbar\partial/\partial\Phi$, and junction capacitance C_s . Here the potential is $U(\Phi, \Phi_x) = (\Phi - \Phi_x)^2/2L + (\Phi_0 I_c/2\pi) \cos(2\pi\Phi/\Phi_0)$, with critical current I_c , applied flux Φ_x , and flux Φ linking the loop.
 - [21] T.P. Orlando *et al.*, Phys. Rev. B **60**, 15398 (1999).
 - [22] Yu-xi Liu *et al.*, Phys. Rev. Lett. **95**, 087001 (2005).
 - [23] D. Vitali *et al.*, Phys. Rev. A **57**, 4930 (1998); Yu-xi Liu *et al.*, e-print quant-ph/0506016, Phys. Rev. A, in press (2005).
 - [24] Yu-xi Liu, L.F. Wei, and F. Nori, Europhys. Lett. **67**, 874 (2004); Phys. Rev. B **72**, 014547 (2005).
 - [25] J.Q. You *et al.*, Phys. Rev. B **71**, 024532 (2005).
 - [26] P. Bertet *et al.*, cont-mat/0412485.
 - [27] Y. Yu *et al.*, Phys. Rev. Lett. **92**, 117904 (2004).
 - [28] For the single-junction flux qubit Hamiltonian [20], the potential $U(\Phi, \Phi_x)$ is not a center of inversion symmetry for variable Φ at the optimal point $\Phi_x = \Phi_0/2$, all microwave-assisted transitions among the three lowest states are possible. Thus, the TDMF-controlled qubit-DB interaction can be performed at the optimal point (e.g., $\Omega_l \neq 0$ when $\Phi_x = \Phi_0/2$). For

the charge-flux qubits [5], we can obtain the same result as the single-junction flux qubits.

[29] Yu-xi Liu *et al.*, cond-mat/0507496.